www.crt-journal.org

CRYSTAL Research & Technology

WILEY-VCH

Wiley Online Library
Early View publication on www.wileyonlinelibrary.com
(issue and page numbers not yet assigned;
citable using Digital Object Identifier – DOI)
Cryst. Res. Technol., 1–9 (2015) / DOI 10.1002/crat.201500061

CRYSTAL Research & Technology

Original Paper

Tracking atomic processes throughout the formation of heteroepitaxial interfaces

Kurt Scheerschmidt[1,*] *and Oussama Moutanabbir*[2]

Received 28 February 2015, revised 18 April 2015, accepted 19 April 2015
Published online 15 May 2015

Understanding the atomic processes governing the formation a heteroepitaxial interface is central to predict and control the basic physical and chemical properties of a variety of hetero-structures. With this perspective, we address in this work the dynamic behavior of Ge atoms deposited on Si-surfaces by molecular dynamics simulations using enhanced bond order potentials. We demonstrate that the deposition of Ge atoms on Si surface induces the competition between several processes including adsorption, desorption, and bulk and surface diffusion involving atomic exchange, substitution, and clustering. By tracking these process, the simulations provide unprecedented insights onto the assembly of the first atomic layer of Ge on Si, the nucleation, growth, and relaxation of islands and quantum dots as well as of defect generation in the bulk.

1 Introduction

Surface phenomena play a crucial role in defining the nature and the quality of hetero-epitaxial interfaces and nanostructures, cf., e.g., [1]. Recent morphological and spectroscopic studies combining low energy electron microscopy and x-ray photoemission electron microscopy of Ge evaporated on Si using molecular beam epitaxy (MBE) demonstrated characteristic temperature dependency of atom exchange processes [2]. It emerges from these studies that the monolayer (ML) growth is nearly abrupt below and at 200 °C indicative of a very limited Ge-Si exchange at this temperature range. However, an increase in growth temperature (>200 °C) triggers intermixing thus leading to a smeared out interface during heteroepitaxy. Developing an atomistic understanding of such phenomena is crucial to control the epitaxial growth of a variety of thin films and nanoscale structures. Due to their technological importance, tremendous effort has been expended to investigate hetero-epitaxial processes such as island and layer growth, and defect generation and migration using various experimental methods. For instance, Ge-Si intermixing in self-assembled quantum dots (QDs), nanoscale structures, and ultra thin layers throughout Ge deposition on Si has attracted a great deal of attention as a model system to elucidate subtle but important atomic-scale processes governing early stages of heteroepitaxy [3–19].

In general, the nature of epitaxial growth is determined by the interplay between several dynamic processes such as adsorption, desorption, intermixing, diffusion on surfaces and into the bulk. In this perspective, molecular dynamics (MD) simulations have been performed to study the atomic processes involved in the early stage of deposition of Ge atoms on Si surfaces. Classical MD simulations are done because of the necessity to use large number of atomes in the models and a large number of time steps to obtain results that are relevant at the nanoscopic or even macroscopic scale. Most of MD simulations are typically carried out by applying the well-known semi-classical potentials of Stillinger-Weber or of Tersoff type. Examples of MD simulations include studies of the intermixing [1, 14, 15], the growth and ordering of Ge islands on Si and SiO_2 surfaces [16–19], the preferred adsorption sites [20, 21], modeling layer growth [22, 23], cluster deposition [24, 25], surface diffusion [26], and reactive effects [27].

Our classical MD simulations cf. Chapter. 2, employ an extended bond order potential (BOP4+) [28–30]. The additional angular terms in BOP4+ describe certain

* Corresponding author: e-mail: schee@mpi-halle.de, Phone: +49-345-5510250, Fax: +49-345-5511223
Dedicated to Professor Dr. Wolfgang Neumann for his 70th birthday
[1] Max Planck Institute of Microstructure Physics, Weinberg 2, Halle (Saale), 06120, Germany
[2] Département de Génie Physique, Polytechnique Montréal, Montréal, C.P. 6079, Succ. Centre-Ville, Montréal, Québec, H3C 3A7, Canada

π-bonding between neighboring atoms and provide higher bond stiffness. The applicability of the bond order potential in structural predictions were demonstrated by recalculating QD relaxations and interface defects [30, 31]. This shows, beyond the limitations of earlier applications [32–37], the importance of structure relaxation in general and for accurate interpretation of the electron microscope images in particular. In addition, the BOP4+ terms enable mimicking the local density, thus including both phase shifts due to dynamic electron diffraction and structural relaxation in mean inner scattering potential calculations for holographic phase-mapping [38]. With respect to the intermixing of Ge-Si, the MD with BOP4+ proved that the energy balance of deposited atoms is the reason for our observations providing evidence for the role of the propagating island edges in atoms swapping across the interface. The calculations demonstrated that substitution of Si by Ge is a low-energy pathway to incorporate Ge in the growing one-atom-thick layer [2]. In the present paper, the atomic processes are investigated in detail by extending the minimization towards dynamic deposition simulations. The MD with BOP4+ is therefore applied to deposit Ge onto Si surfaces and to trace the movement of the deposited atoms and to analyze statistically the resulting structures.

2 Simulations

The MD simulations, solving the Newtonian equations of movement for all particles in the models together with deposited atoms, are performed by applying the enhanced BOP4+ [30–32]. The BOP4+ is based on the tight binding model applying analytically the first four moments of the density which is an extension to order 4 using new on-site and π-terms of the local density of states. The resulting semi-empirical many body potential is transferable to describe phases and features not found in other empirical potentials. Moreover, transferability extends to different kinds of materials, where only the parameters need to be refitted. In our implementation of BOP4+ we have retained a number of angular terms related to certain bonds between neighboring atoms ignored previously. All contributions exhibit new angular dependencies. BOP4+ preserves the essential quantum mechanical nature of atomic bonding and achieves O(N) scaling (order N, i.e. linear with number of particles) by diagonalizing the tight-binding Hamiltonian recursively. This enables fast and accurate MD simulations on macroscopic time and length scales beyond the realm of the *ab initio* calculations.

The simulations were performed using different configurations of super-cells (SC) and a wide variety of tempering and deposition conditions, cf. figures 1 and 2. The SC's are developed by transforming a Si-unit cell into an orthogonal cell where the surface of interest, i.e., surfaces with ⟨100⟩ or ⟨111⟩ type of normal direction, is within one of the SC low indexed directions. The transformed orthogonal unit cells are enlarged by multiples of the unit cell lengths and cutting out the free surfaces and elongating the box orthogonal to the surfaces to get sufficient empty space above the surfaces for the additional Ge-atoms to be deposited. The models have either flat surfaces or flat islands or pyramidal QD structures on top. In addition, the Ge/Si mixture is varied on top, especially in the flat island, where some of the prerelaxed structures of [2] are used as start models, too. The SC's used are as follows:

SC1a,b:	1.6292 nm*1.6292 nm*(3.2 nm or 5.2 nm), 216 atoms, {100} or {111} surface,
SC2a,b:	(2.83 or 3.83)nm*2.3041 nm*3.9907 nm, 896 atoms, {111} surface,
SC3:	7.9814 nm*4.61082 nm*4.8219 nm, 3584 atoms, {111} surface,
SC4:	(7.0577 nm)**3, 10478 atoms, {100} surface,
SC5a,b:	(23.124 nm)**3, 312666 or 551165 atoms, half-filled SC without and with pyramidal free standing QD on top, {100} surface,
SC6a,b:	19.9535 nm*19.2005 nm*30 nm, 358000 atoms or 31.9256 nm*18.4328 nm*50 nm, 655312 atoms, {111} surface.

For all configurations MD simulations are performed using different treatment as described later on. The results are all included in figure 11 summarizing all simulations. For the sake of clarity in figures 3–10 only three examples with small extensions are discussed in detail.

Figure 1 shows from left to right two SC2b with {111} surfaces and one SC5b structure with a {100} surface. The first SC2b has a flat island on top consisting of solely Ge, the second, with a bilayer island is one of the prerelaxed structures from [2]. The large SC5b has a pyramidal free standing QD on top with {110} facetted and a two-atomic wetting layer.

The MD simulations are all done applying isobar-isothermal (NpT) conditions, i.e., constant pressure and constant particle number are assumed in every relaxation step of around 10 ps (1000 to 10000 MD-steps of 0.5 fs) to rescale the particles momenta back to get a fixed bulk temperature. The rescaling of the velocities is done either by hard scaling or according to the Berendsen-thermostat [28]. The integration time step

CRYSTAL Research & Technology

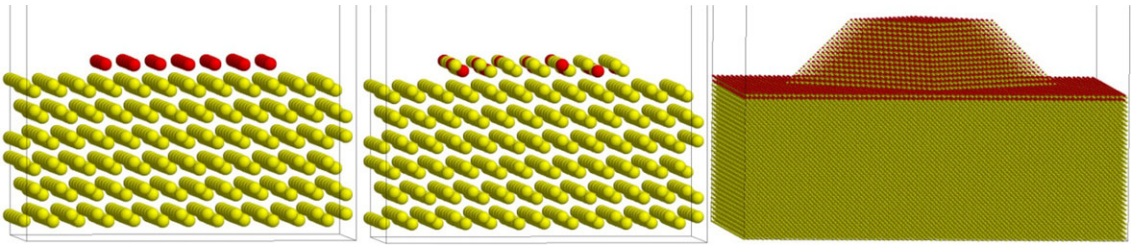

Fig. 1 Initial configurations (from left to right, resp.) of type {111}-SC2b with a monolayer island of pure Ge, a SiGe -bilayer island, and a large {100}-SC5b with a pyramidal QD on a two atomic wetting layer.

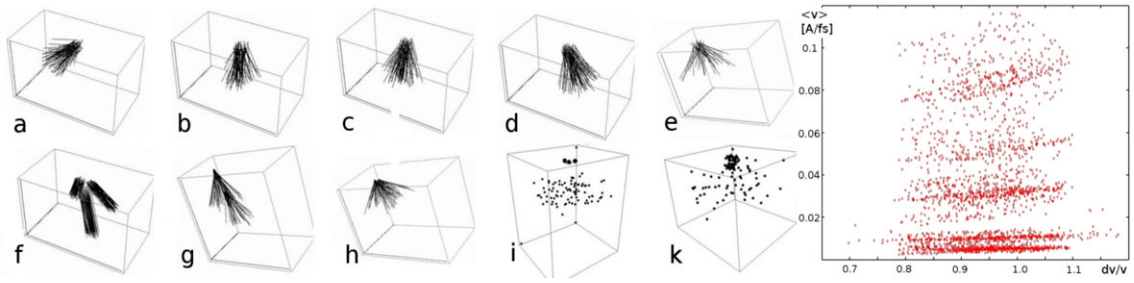

Fig. 2 Some typical distributions (a-k, for details, cf. text) of the deposited Ge atoms at random start position, angular and velocity distributions indicated by the direction and length of the strikes or by dots for begin and end of the trajectories, and random distribution probability of δv/v versus v at the right hand side of the figure.

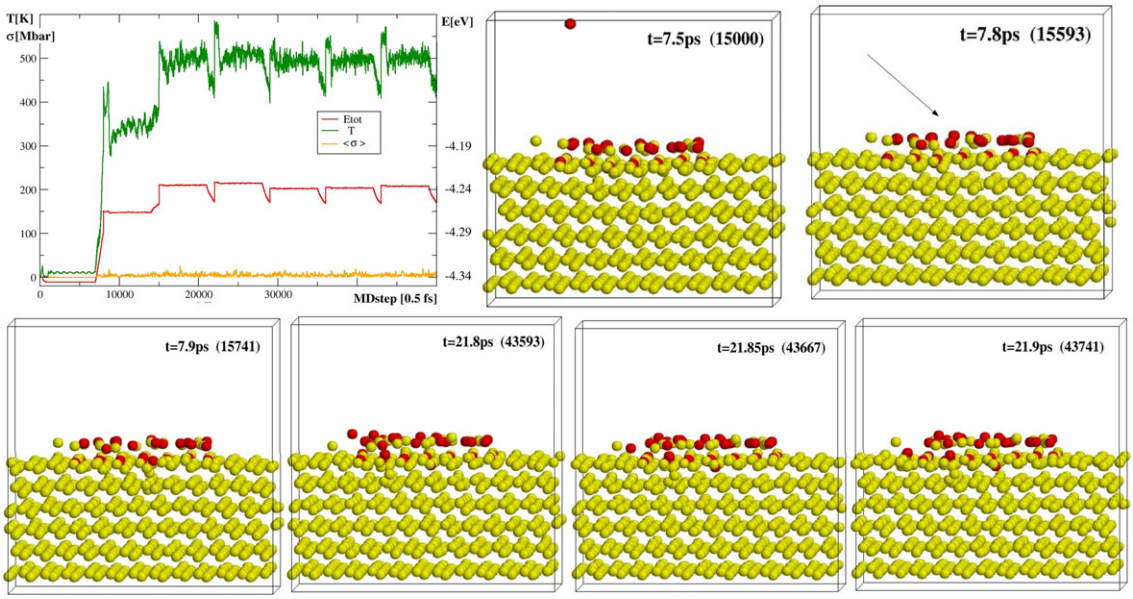

Fig. 3 Temperature T(K), total energy per atom E(eV) and bulk modulus σ (Mbar) for the first 50000 steps (10 ps) of MD simulated deposition of Ge (red) onto {111}-Si surface with mono-atomic SiGe-island (configuration SC2b) and selected snapshots, starting at 7.5 ps (step 15000) with one additional Ge after relaxation at 400 K, and sequences (around 7.8 and 21.8 ps) where atoms attaches surface and rim of the island, and showing exchange underneath the island.

of 0.5 fs is chosen to get sufficient stability of the surfaces. After relaxing the initial models, at a few hundreds K, additional Ge atoms are deposited with varying energy and momentum randomly. A maximum of three Ge atoms are deposited at a time, then the whole system is relaxed again 1000 steps or more. The deposited Ge must be positioned without small distances at start to prevent high particle momenta due to repulsion. Figure 2 shows schematically fans of deposition trajectories as applied in the simulations with varying start positions,

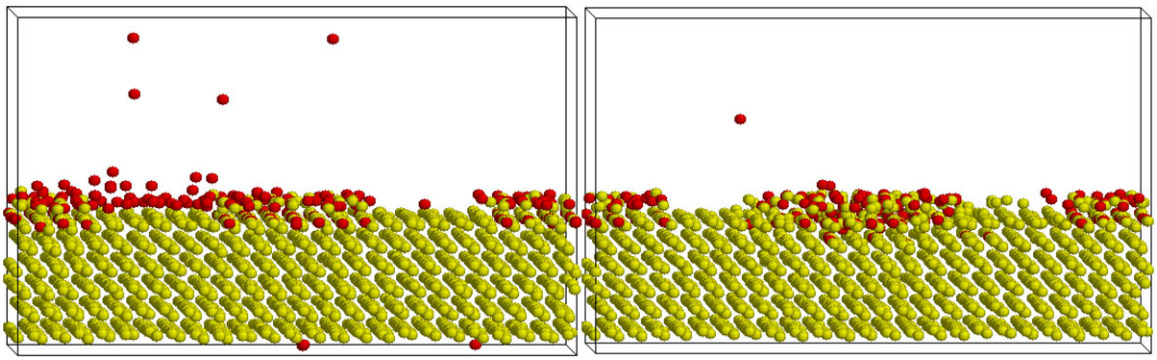

Fig. 4 Snapshots at 30 ps of the Ge-deposition onto {111}-Si surfaces with SiGe island (configuration SC3) demonstrating layer growth between the islands (left) and island growth (right) for the cases (i, $T_{depo} = 1000$ K, $T_{bulk} = 500$ K) and (ii, $T_{depo} = 6000$ K, $T_{bulk} = 400$ K), respectively.

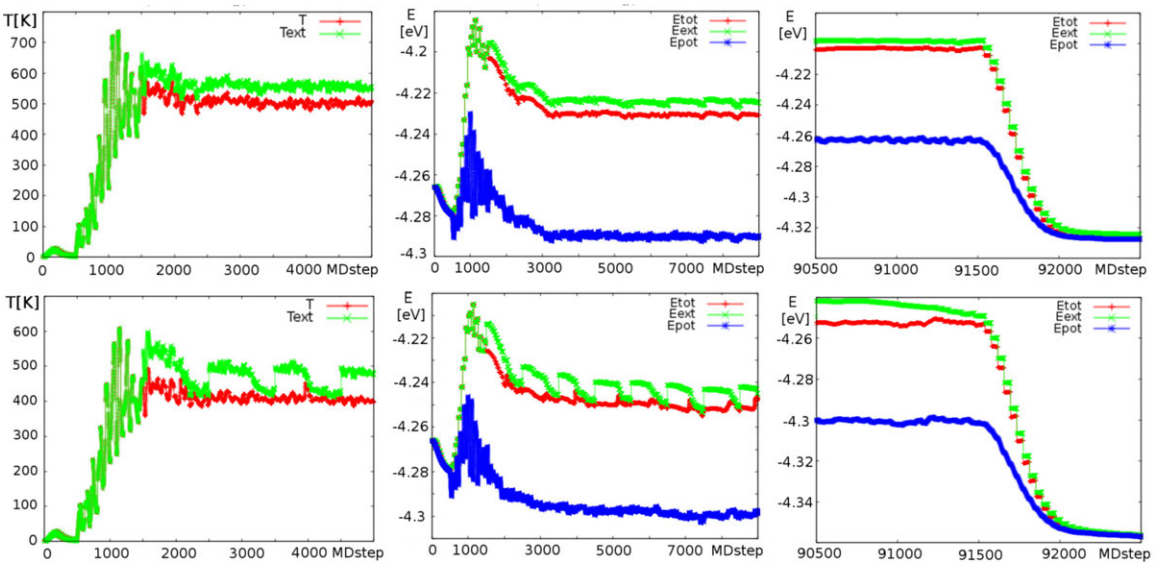

Fig. 5 Temperatures at the beginning and energies at beginning and end of a typical MD simulation: Ge deposition onto a Ge-Si island on top of {111}-Si-surfaces (MDstep = 0.5 fs; upper/lower row correspond to case i/ii of figure 4, i.e. $T_{bulk} = 500$ K and 400 K, resp.; isotherm-isobar conditions): Temperatures T_{tot}(K) and T_{ext}(K) (cf. text) are resulting from the differences between total and external energy E_{tot}(eV), E_{ext}(eV) to the potential energy E_{pot}(eV). The energy E_{ext} of the deposited external atoms is given by the velocity of the deposited Ge.

different fan inclination α (approx. ⟨101⟩ in figure a, ⟨001⟩ in figure b,e,g,h,k, ⟨019⟩ in figure c,⟨109⟩ in figure d,f,i) average velocities v as well as velocity δv and angular $\delta\alpha$ distributions. The particle velocity distributions δv vary between 0.3 and 1.5 fold of the mean values v[Å/fs] = 0.005, 0.01, 0.03, 0.05, 0.08 corresponding to deposition temperatures of T_{depo} between 600 K and 10^4 K for the starting Ge deposits (cf. random distribution δv/v versus v at the right hand side of figure 2). The approximative values used in the examples of figure 2 are v[Å/fs] = 0.001(e), 0.005(a), 0.01(b,c,d,f,i), 0.03(g,h,k), $\delta\alpha$ = 0.3(a-d,g), 0.5(e,f), 0.7(h,i), 1.(k), and δv/v = 0.3(a,c,d), 0.4(b,g), 0.5(e,f,h), 1.1(i), 1.5(k).

To describe the early stage of the hetero-epitaxial growth including surface diffusion, mixing and exchange of atoms as well as the assembly of two-dimensional islands, calculations of atomic displacements, potential energy, stress, and temperature were carried out by averaging over a few hundreds integration steps. The system was allowed to equilibrate, both geometrically and compositionally, before being subjected to annealing until a given temperature is reached. Herein, T_{bulk} is varied from 100 K to 600 K increasing in 100 K annealing step. During the cooling, the system relaxes through atomic displacements and volume changes, which are measured by the change of the

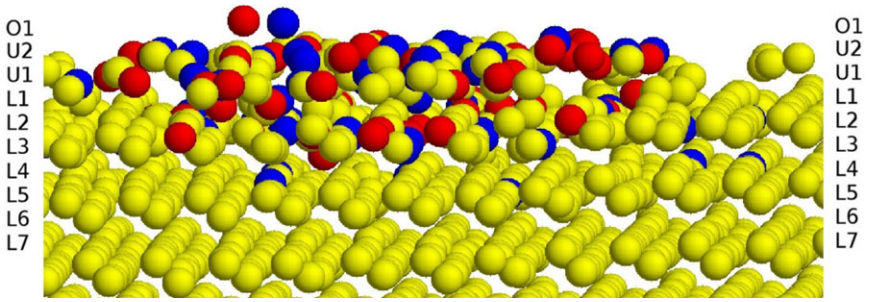

Fig. 6 Details of the growth of the Ge island of case (ii) from figures 4 and 5 (deposited Ge-atoms in blue, Si yellow, non deposited Ge red) with defects in the island and ex-change processes in layers underneath the island, too. The layer-legend O, U and L characterize the half-atomic layers of the free surface, upper island and bulk layers, resp., as used in analysis (cf. text).

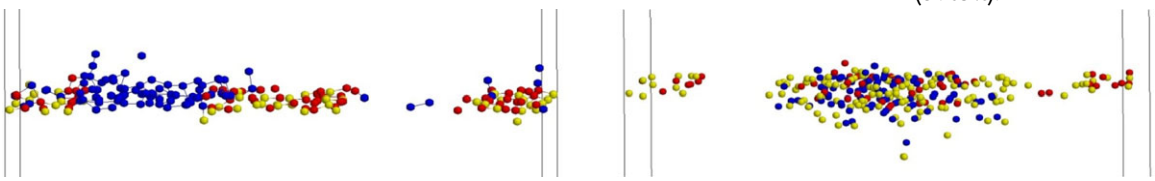

Fig. 7 Deposited Ge (blue) and all Si (yellow) and Ge (red) shifted more than 5% out of the start position of cases (i left,ii right) of the MD-step shown in figure 4, i.e., the number of shifted atoms is a criterion for the strain remaining within the SC after deposition and relaxation of the additional Ge atoms.

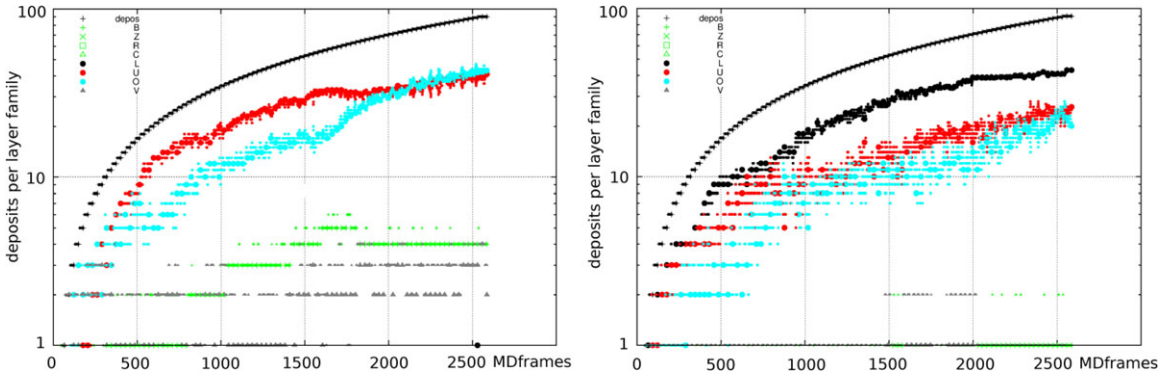

Fig. 8 Layer family analysis of all 2500 movie frames each of 36 MD steps (18 fs) in logarithmic presentation. The curve of grey crosses reflects all deposited particles, i.e., every 1000 MD-steps (0.5 ps) the number of deposited Ge-atoms is increased by one. The larger symbols for every 90 frames show the configuration for the deposition events numbered with respect to the layer family. The smaller symbols demonstrate the behavior of the deposits during the 0.5 ps relaxation between the depositions, like diffusion between the layers etc. At the beginning 500 static and 1000 dynamic relaxations are performed before the deposition starts. For case i (left) the most of the deposits are placed in O and U, for case ii (right) the upper bulk layers L get the most deposits.

SC axes and registered as the relative volume change dV/V.

Figure 3 shows the variation of temperature, total energy, and bulk modulus for the first 25 ps of the MD simulation (SC2b, with constant NpT) along with selected snapshots for surface reordering while depositing Ge atoms. After relaxation of the SiGe island on the {111}-Si surface at 0 K and heating up to 400 K, starting at t = 7.5 ps (step 15000) every 3.5 ps (7000 steps) one additional Ge is deposited with varying energy and momentum (case h of figure 2 with v = 0.03 Å/fs). Two of different reaction paths are selected here, at 7.8 ps the Ge is deposited below the island in the next layer pushing away neighbor atoms, while at 21.9 ps the Ge becomes attached to the island edge. In addition Si-Ge exchange underneath the island can be observed.

3 Results

By following the trajectory of Ge atoms on Si surfaces in MD-simulations the effects of deposition, diffusion, ad- and desorption can directly be studied. However, to get quantitative results, the resulting configurations after a large number of depositions have to be analyzed. Figure 4 shows two snapshots at 30 ps for differently

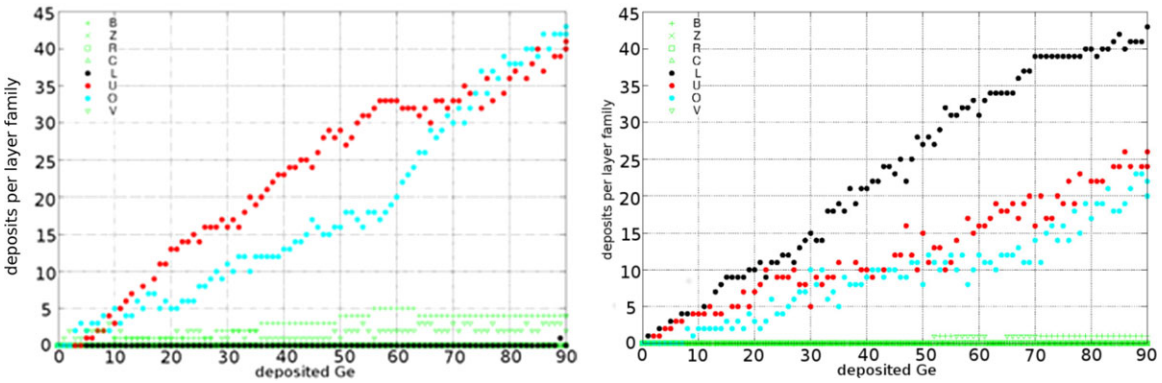

Fig. 9 Layer family analysis for all deposition events for the cases (i left, ii right), i.e., particles per layer family as function of the number of deposited Ge atoms in linear presentation. Comparing the different grouping the particle movement, especially layer mixing and exchange, can be seen at a glance: i) after approximately 70 deposits the islands are overgrown (O > U), ii) due to the higher T_{depo} the most of the deposited Ge are placed in the upper bulk layers L.

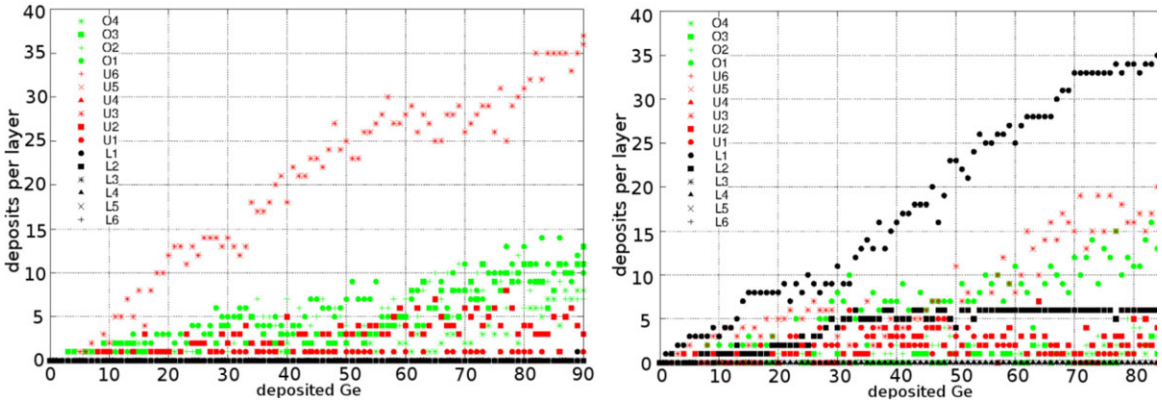

Fig. 10 Layer analysis as in figure 9 for selected layers near the top surface for the cases (i left, ii right): i)the most deposits are placed in U3 (growth between islands) or distributed over O1-O4(island overgrowth), ii) the deposits are placed in L1 and diffuse with increasing simulation time into L2.

developing systems after the same number of deposited Ge-atoms onto the same starting configuration (SC2a) with two SiGe islands on top of Si-{111} surface. After static relaxation at 0 K, followed by 500 steps dynamic relaxation at 0 K the systems are heated up to 500 K and 400 K within 1000 steps in case (i) and (ii), respectively. Without fixing the basic layer, strained regions occur below the islands and crinkling of the whole structure. Direction and distribution of the deposited Ge as applied for case (i) and (ii) in figure 4 is given by figure 2a and figure 2c, respectively, which can be characterized as: (i) $T_{depo} = 1000$ K, $T_{bulk} = 500$ K, inclined incidence, (ii) $T_{depo} = 6000$ K, $T_{bulk} = 400$ K, deposition on top of the island. Here, T_{bulk} is the temperature of the bulk thermostat, which reflects the difference between the total and the potential energy E_{pot}-$E_{tot} = E_{kin} \sim kT$, and T_{depo} describes the average of the random deposition as explained above.

Figure 5 shows the energies for the first 9000 and the last 2000 steps which describes 4.5 ps from the beginning and 1.0 ps of the down-cooling at the end of the MD simulation. During the whole run of 92500 steps, i.e. 46.25 ps of alternating deposition and MD-relaxation, every 1000 steps one Ge atom is deposited and T_{bulk} rescaled. The deposition is described energetically by E_{ext} and the corresponding T_{ext} which characterizes the external excess energy brought by the kinetic energy of the deposit into the system. The energy difference of approximately 0.005 eV and 0.1 eV for cases (i) and (ii), respectively, is the kinetic energy of the actual deposit. The related temperature difference T_{ext}-T_{tot} is due to the relative energies by the factor square root of the particle number smaller than T_{depo}. After every deposit the system is rescaled which thermalizes the deposited atom, indicated by T_{ext} approaching T_{tot}, however, the rescaling requires sufficient time to avoid freezing of the deposits

CRYSTAL Research & Technology

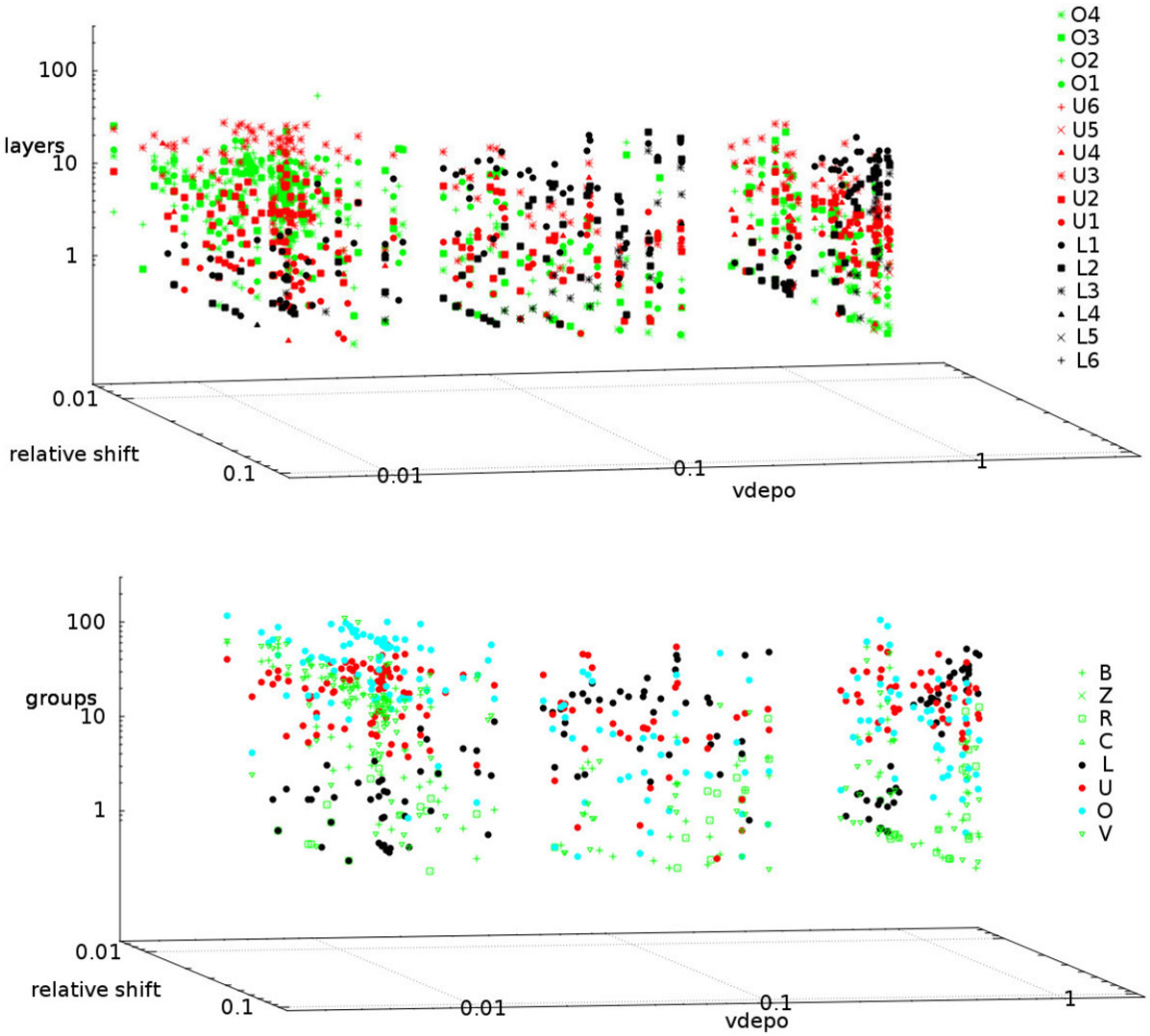

Fig. 11 Statistics over all MD-deposit simulations: The deposited Ge in different layers or layer family (upper/lower figure, resp.)as function of the relative number of 5% displaced species and the deposition velocity v_{depo} (deposition temperature T_{depo}): with increasing T_{depo} the deposits are placed deeper into the bulk and this is related to increased remaining strain characterized by the higher relative number of 5% shifted atoms.

before interaction with the bulk. Figure 5 thus explains the effects observed in figure 4. The most remarkable effect in the examples of figure 4 is the layer growth between the islands for the inclined incidence and the low deposit velocity in case (i), whereas the normal deposition at higher temperatures in case (ii) results in island growth.

Figure 6 shows the higher impact onto the island in case (ii) in more detail and by coloring the deposited atoms blue for better discriminating them. Some exchange and mixing effects can be seen directly. The complete diffusion processes, adsorption and desorption as well as the atom exchange and intermixing, however, may better be seen looking for the movies registered during the MD simulations, cf. mpeg-examples at web-page [39], instead of analyzing the snapshots in figures 4–6.

4 Discussion

To get a better overview of the results of the MD simulations all atomic trajectories visualized in the movies are analyzed by a statistical method as described in the following. The whole structure is divided into layers as indicated in figure 6. The bulk region is separated into the layers Ln near the top surface and Rn near the rear one, which reflects the stacking sequence along the deposition direction. The maximum slab numbers chosen are

n < 10. Possibly remaining compact layers of the SC between L9 and R9 are denoted by C (as seen later, only a marginal number of deposits is placed in compact inner layers C). Layers of islands or other structures on top/bottom are denoted by Un/Zn and surface atoms on front/back side by On/Bn. Remaining, possibly frozen or not yet bonded deposits are numbered by V (vacuum atoms).The thickness of the layers On,Un,Ln,Rn,Bn,Zn (from top to bottom) reflects the stacking sequence and is therefore different for ⟨100⟩ and ⟨111⟩ surfaces. The number of On and Un layers depend on the island structure generated onto the bulk. In addition, all atoms are registered, which are more than 5% shifted out of its position in the start configuration, cf. in figure 7 the situation for the MD-step discussed in figure 4. Figures 8–10 show some details of the layer analysis: figure 8 the layer family analysis for all registered frames in logarithmic presentation, figure 9 layer family for every of the 90 deposition events, and figure 10 the same for selected layers. Grouping in a family means L = L1+L2+ . . . L9 (simile for U, O, etc); the 2500 frames in figure 8 reflect the dynamic behavior every 18 fs, i.e., the detailed particle movement during relaxation, indicated by the small symbols. Every 1000 MD-steps (= 0.5 ps) a Ge is deposited, indicated by the larger symbols in figures 8–10, i.e. the whole MD simulation covers 90000 steps (= 45 ps).

At a glance the group and layer statistics show the pathway for the particles from and along the surfaces, hopping forth and back, and moving towards deeper layers. The most important factor controlling this behavior is the impact energy described by T_{depo}, as the cases (i) and (ii) reflect comparing the U vs O and L groups as well as the U3 and L1 layer statistics, etc. The detailed behavior is described in the figure captions of figures 9 and 10. As can be seen, the deposited Ge are placed into U3,O1, O2,U2 in case (i), and L1, U3, O1 and L2 in case (ii). The effects are related to diffusion and intermixing processes, whereas the not shown exchange between V and O or U layers describe the ad-and desorption processes.

The statistics over all simulated examples is given in figure 11 as function of two selected simulation parameter, the deposition velocity v_{depo} (deposition temperature T_{depo}) and the relative number of 5% displaced species. Both, the representation of selected layers and the layer family analysis demonstrate that with increasing T_{depo} the deposits are placed deeper into the bulk and this is related to increased remaining strain characterized by the higher relative number of 5% shifted atoms. For v_{depo} < 0.03 the most of the deposits are at or near the surface in O and U layers, for v_{depo} > 0.08 the number of deposits in L1 and L2 layers is remarkably increased. For Ge the thermic velocity v_{depo} = 0.04 Å/fs corresponds very roughly to T_{depo} = 500 K, however, as discussed above, the applied T_{depo} depends on the scaling of T_{bulk} during the MD-simulations.

5 Conclusions

Varying MD and deposition conditions unraveled an ensemble of processes governing the early stage of hetero-epitaxy including surface diffusion, the mixing and exchange of atoms as well as the assembly of two-dimensional islands. The simulated position of Ge atoms on a Si(111) surface demonstrates the nucleation of alloyed ML-high 2D islands with very negligible adsorption on bare Si (less than 1% of deposited atoms), intermixing is found to be predominantly confined in the two topmost layers, in agreement with experimental findings. The lower surface diffusivity and denser double-layer structure of Si(111) may be at the origin of this limited mixing as opposed to Si(100), where Ge can reach down the fourth layer.

References

[1] T. Leontiou, J. Tersoff, and P. C. Kelires, Phys. Rev. Lett. **105**, 236104 (2010).
[2] O. Moutanabbir, F. Ratto, S. Heun, K. Scheerschmidt, A. Locatelli, and F. Rosei, Phys. Rev. **B85**, 201416 (2012).
[3] O. Moutanabbir, S. Miyamoto, E. E. Haller, and K. M. Itoh, Phys. Rev. Lett. **105**, 026101 (2010).
[4] S. Miyamoto, O. Moutanabbir, T. Ishikawa, M. Eto,E. E. Haller, K. Sawano,Y. Shiraki, and K. M. Itoh, Phys. Rev. **B82**, 073306 (2010).
[5] J. Stangl, V. Holý, and G. Bauer, Rev. Mod. Phys. **76**, 725 (2004).
[6] O. Moutanabbir, Sci. Adv. Mater. **3**, 312 (2011).
[7] Y. Tu and J. Tersoff, Phys. Rev. Lett. **98**, 096103 (2007).
[8] M. H. von Hoegen, B. H. Müller, T. Grabosch, and P. Kury, Phys. Rev. **B70**, 235313 (2004).
[9] R. Ditchfield and E. G. Seebauer, Phys. Rev. Lett. **82**, 1185 (1999).
[10] V. A. Yuryev, L. V. Arapkina, M. S. Storozhevykh, V. A. Chapnin, K. V. Chizh, O. V. Uvarov, V. P. Kalinushkin, E. S. Zhukova, A. S. Prokhorov, I. E. Spektor, and B. P Gorshunov, Nanoscale Res. Lett. **7**, 414 (2012).
[11] G. Biasiol and S. Heun, Phys. Rep. **500**, 117 (2011).
[12] G. H. Gilmer, H. Huang, and Ch. Roland, Comput. Mater. Sci. **12**, 354 (1998).
[13] S. Kowarik, K. Broch, and F. Schreiber, Phys. J. **13**, 33 (2014).
[14] R. J. Wagner and E. Gulari, Phys. Rev. **B69**, 195312 (2004).

[15] F. Montalenti, A. Marzegalli, G. Capellini, and M. de-Seta, J. Phys. Condens. Matter. **19**, 225001 (2007).
[16] R. Marchetti, F. Montalenti, L. Miglio, G. Capellini, M. De Seta, and F. Evangelisti, Appl. Phys. Lett. **87**, 261919 (2005).
[17] Kh. B. Ashurov, F. Djurabekova, S. E. Maksimov, A. I. Nikiforov, S. Tadjimuratov, and B. L. Oksengendler, Nucl. Instrum. Methods Phys. Res. B **282**, 38 (2012).
[18] P. Ashu and C. C. Matthai, Appl. Surf. Sci. **56–58**, 661 (1992).
[19] C. Y. Chuang, Q. Li, D. Leonhardt, S. M. Han, and T. Sinno, Surf. Sci. **609**, 221 (2013).
[20] C. H. Grein, R. Benedek, and T. dela Rubia, Comput. Mater. Sci. **6**, 123 (1996).
[21] D. Srivastava, B. J. Garrison, and D. W. Brenner, Langmuir **7**, 683 (1991).
[22] St. Ethier and L. J. Lewis, J. Mater. Res. **7**, 2817 (1992).
[23] H. W. Lu, J. Q. Xie, and J. Y. Feng, Nucl. Instrum. Methods Phys. Res. B **170**, 71 (2000).
[24] A. Harjunmaa, J. Tarus, K. Nordlund, and J. Keinonen, Eur. Phys. J. **D 43**, 165 (2007).
[25] Chen Zhi-Hui, Yu Zhong-Yuan, Lu Peng-Fei, and Liu Yu-Min, Chin. Phys. **B18**, 4591 (2009).
[26] M. Z. Hossain, J. B. Freund, and H. T. Johnson, J. Appl. Phys. **111**, 103513 (2012).
[27] A. Barbato and C. Cavallotti, Phys. Stat. Sol. **B247**, 2127 (2010).
[28] K. Scheerschmidt, in: Theory of Defects in Semiconductors, D. A. Drabold and S. Estreicher (Eds.), Topics in Applied (Physics Springer, Verlag, 2006), Chapter 9, pp. 213–244.
[29] V. Kuhlmann and K. Scheerschmidt, Phys. Rev. **B76**, 014306 (2007).
[30] K. Scheerschmidt and V. Kuhlmann, Int. J. Mat. Res. **98**, 11 (2007).
[31] T. Wilhelm, V. Kuhlmann, and K. Scheerschmidt, Phys. Status Solidi C **4**, 3115 (2007).
[32] H. Blanck, D. Litvinov, R. Schneider, D. Gerthsen, T. Passow, and K. Scheerschmidt, Cryst. Res. Technol. **44**, 1083 (2009).
[33] K. Scheerschmidt, D. Conrad, H. Kirmse, R. Schneider, and W. Neumann, Ultramicroscopy **81**, 289 (2000).
[34] H. Kirmse, R. Schneider, K. Scheerschmidt, D. Conrad, and W. Neumann, J. Microsc. **194** 183 (1999).
[35] S. Ruvimov and K. Scheerschmidt, Physica Status Solidi (A) **150**, 471 (1995).
[36] K. Scheerschmidt and P. Werner, Characterization of structure and composition of quantum dots by transmission electron microscopy, in: Nano-Optoelectronics: Concepts, Physics and Devices, M. Grundmann (Ed.) (Springer-Vlg., Bln., Heidelbg., New-York , Tokyo, 2002), Chapter 3, pp. 67–98.
[37] K. Scheerschmidt and V. Kuhlmann, Microsc. Microanal. **13**(Suppl. 3), 22 (2007).
[38] C. L. Zheng, K. Scheerschmidt, H. Kirmse, I. Häusler, and W. Neumann, Ultramicroscopy **124**, 108 (2012).
[39] http://www.mpi-halle.mpg.de/~schee/filetransfer/SiGedata